AN ELLIPSOMETERIC EVALUATION OF ION IMPLANTED SILICON

Patrick G. Drennan
Senior Microelectronic Engineering Student
Rochester Institute of Technology

ABSTRACT

A Split Split Plot Design was implemented to investigate the relationship between the ion implantation conditions and the complex refractive index of the inherent damage layer. Four factors chosen to evaluate this relationship were wafer orientation, dose concentration, implant acceleration potential, and screen oxide thickness. The response variable was the complex refractive index of the damaged layer measured by ellipsometry. Results indicate that there is a relationship between the dose concentration and the response variable that is most sensitive to doses between 5e13 ions/cm2 and 5e15 ions/cm2. However, the range of the refractive index increases considerably in this range to prevent the implementation of this method as an evaluation tool.

INTRODUCTION

When high molecular weight particles are implanted into silicon wafers, a layer of damage is created across the surface due to physical collisions between the bombarding species and the silicon atoms [1-6]. Dislocations of these atoms result in an amorphous layer in which the refractive index has been altered from the monocrystalline silicon. As such, an optical measurement tool that is highly sensitive to this change, such as an ellipsometer, may be used to measure the new refractive index this amorphous layer [7-11]. In this experiment, the measured samples were treated as substrates without a thin film present and the complex refractive index was obtained. Treating the amorphous layer as a substrate, the ellipsometer routines can determine the complex refractive index of the film and hence the amount of damage created by the implantation.

In null ellipsometry, a collimated monochromatic light source passes light through a polarizer and a quarter wave plate which act together to form an ellipsometerically polarized beam of light. When reflected from a surface, the ellipticity of this beam is altered. To determine the change in the ellipticity, another polarizer is placed before a photodetector and is rotated until a minimum or zero intensity is measured at the photodetector. The angles of the two polarizers and the quarter wave plate can then be used to calculate the change in phase

(delta) and in magnitude (psi) of the reflected beam. These values, in turn, may be used to find the complex refractive index of the substrate or the thickness and refractive index magnitude of a thin film.

Upon implantation, the optical and physical alterations to the wafer surface are related to the nature of the ion implantation conditions. Parameters such as acceleration potential, species, dose concentration, and channeling should have an effect on the refractive index. These relationships may then be derived and implemented to calculate or estimate the aforementioned implantation parameters.

In terms of practical application, a nondestructive technique for evaluating ion implantation dose concentration and uniformity is an attractive proposition particularly with the lower dose implants (ie threshold voltage adjust implants -- ~5e11 cm-2). Not only would this technique provide real time analysis, which is instrumental in instituting statistical process control, but it may also provide for retroactive dose corrections and eliminate an anneal cycle that is required for four point probe measurement. In this work, an investigation of the potential for an ellipsometeric evaluation of ion implantation was performed.

EXPERIMENT

Based upon prior knowledge of ion implantation damage creation, it was decided that the four most influential factors on the damage creation were dose concentration, crystal orientation, screen oxide thickness, and acceleration potential [1,8]. With this in mind, a Split-Split Plot Design was developed in order to minimize the number of wafers employed while maintaining a sufficient number of treatment combinations so that this system may be adequately characterized. The experimental matrix appears as Figure 1. The factors Crystal Orientation and Acceleration Potential had levels of <100>, <111> and 50, 125, and 200 keV, respectively. Within each of these treatment combinations were two wafers for replication so that the between wafer variability could be estimated.

As labeled in Figure 1, within each wafer, the wafer was split in half. One half of the wafer had a screen oxide while the other half did not. Perpendicular to the separation of the screen oxide, were five bars of implantation ranging from doses of 3.0e11 to 3.0e15 ions/cm2, incremented in orders of magnitude. These doses were randomly distributed amongst these five bars, but every wafer contain each of the five doses for a total of ten experimental units per wafer. Ion implantations were masked with conventional positive NDS/Novolac resist spun onto the wafers at 3000RPM for a thickness of approximately 1.5 microns. Wafers were exposed and developed such that only the bar of interest was exposed for the implantation.

Two control wafers were also included in the experimental design. These wafers were implanted at a center point in the matrix both before and after each day of implantation so that day to day variability in the implanter may be measured and removed. These wafers were implanted at a dose concentration of 3.0e13 ions/cm2, crystal orientation of <100>, energy of 125keV, and with no screen oxide present.

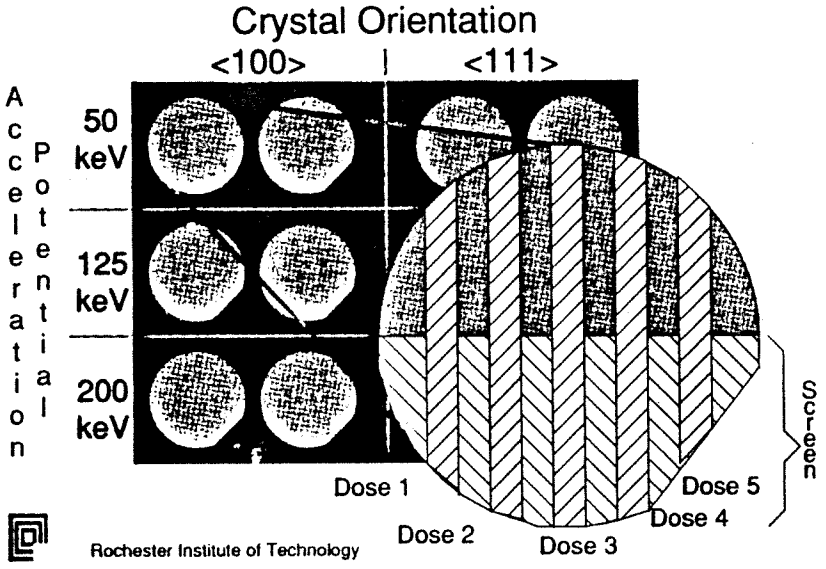

FIGURE 1: Experimental Matrix.

Wafers were implanted on a Varian/Extrion medium current implanter over a span of four days using a BF2 source. Measurements were performed on a CVC/PLASMOS SD2000 nulling ellipsometer.

RESULTS/DISCUSSION

Alterations in the refractive index of the wafers after implantation were apparent to both the naked eye and ellipsometry. Ellipsometeric measurements were performed by treating the wafers as substrates without a thin film present on the surface so that the real and imaginary components of the refractive index could be measured, as opposed to just the magnitude. Also, when treating the damaged layer as a thin film over a crystalline silicon substrate, it was theorized that the ellipsometer would likely incur some difficulty in determining the interface between the damaged layer and the substrate since the damage is placed over some single sided distribution.

The analysis of variance for both components of the refractive index is shown in Table 1. Under the column labeled 'Source', E is the acceleration potential, O is the crystal orientation, S is the screen oxide thickness, and D is the dose concentration. The terms labeled W are the error terms used to calculate the F ratio as labeled in column 5. The terms with a

star (*) are interactions between the factors listed in that term. Fourth order interactions were not investigated. The last column is the alpha value needed to accept the null hypothesis that there is statistically no difference between the levels of a given source. In other words the lower the value in column 6 the higher the impact that that source will have on the refractive index.

Using this information, it was readily apparent that the acceleration potential, dose concentration, and the screen oxide thickness were statistically significant. However there was not sufficient evidence to conclude that the crystal orientation had an impact on the change in refractive index. Therefore, those treatment combinations that varied in terms of orientation alone were considered to be replications and the entire experimental matrix was reduced from four factors to three.

Bearing this in mind, the plots of the real component of the refractive index versus dose concentration are listed in Figure 2 for both screen oxide thicknesses and all three acceleration potentials. Four pieces of information can be extracted from these plots. First, as one increases the acceleration potential, generally speaking, the refractive index increases for the higher doses (3.0e14 to 3.0e15 ions/cm2). This parallels what one might anticipate since the kinetic energy built up during the acceleration must transfer to the silicon substrate and displace some of the silicon atoms from the crystal structure either via inelastic collisions or energy transfer mechanisms. Second, an increase in the dose concentration also was reflected in an increase in the refractive index. This was intuitively apparent since additional energy must be dissipated to the crystal by virtue of the increased number of atoms being implanted. Third, the presence of a screen oxide over the wafer resulted in a smaller impact on the refractive index for higher doses. This was easily accounted for by the energy absorption of the screen oxide which apparently removed a significant portion of the damage from the silicon crystal. And finally, the range of values for the refractive index also increased with increasing dose concentrations.

This last point is demonstrated in Figure 3, where the range in refractive index values is plotted versus the dose concentration for all of the points measured. It was clear to see that both the real and imaginary components follow this trend which appears to be the single greatest flaw in this evaluation methodology. For example, if one measured a wafer with no screen oxide on it that was implanted at 200keV, they might obtain a value for the real component of the refractive index of 4.15. Refering to the bottom left plot in Figure 2, one could not conclude that the wafer was implanted with 3.0e14 or 3.0e15 ions/cm2 or any other value in between. A similar argument could be presented for the imaginary component.

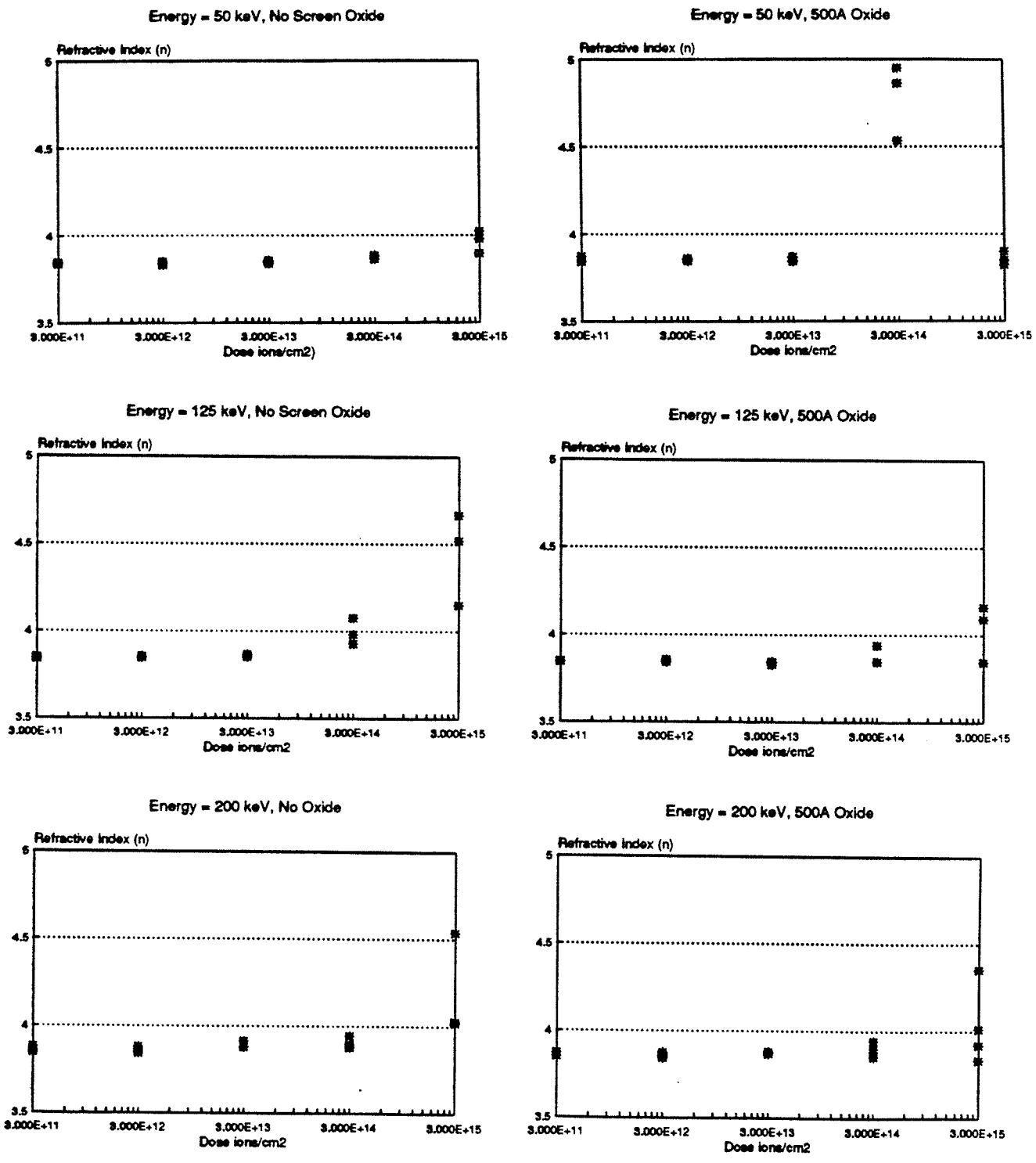

FIGURE 2: Plots of refractive index versus dose concentration.

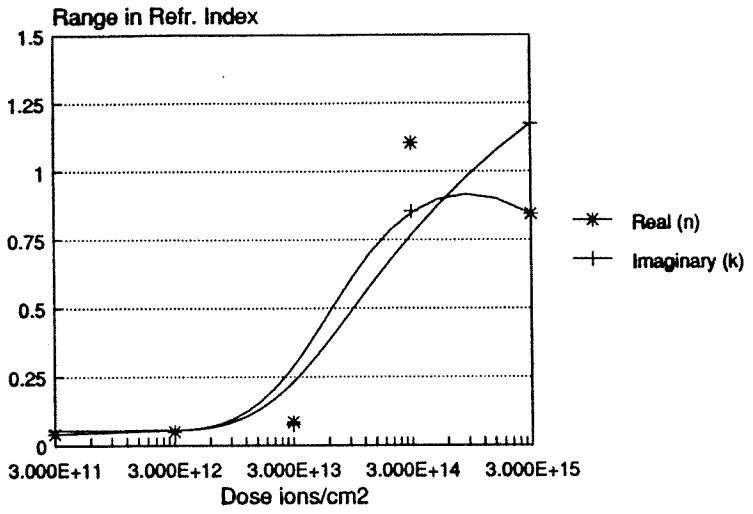

FIGURE 3: Refractive index range versus dose concentration.

It was instructive to visualize both components of the refractive index on a three dimensional plot as shown in Figure 4. Clearly one can see that the outer two most bars of implantation (doses of 3.0e11 and 3.0e12 ions/cm2) are not apparent in these plots. The middle bar (dose of 3.0e13 ions/cm2) shows up only on the imaginary component plot. The two highest doses (3.0e14 and 3.0e15 ions/cm2) had significant impact on both components. It is clear to see to separation of the screen oxide thicknesses, particularly in the imaginary plot. As previously outlined, the range of values for refractive index increased as the values themselves increased. Looking at the highest bar in the real component plot, the variation in these values is considerably greater than the second highest bar. This same point could be observed on the imaginary component plot if the angle of view had been chosen properly.

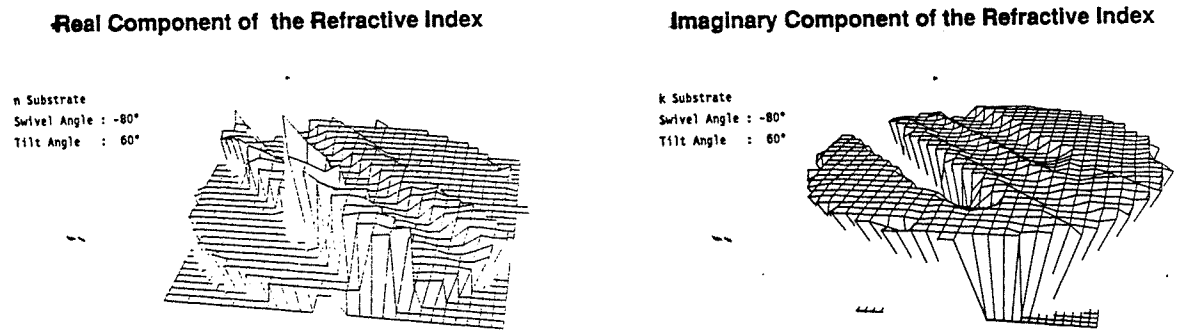

FIGURE 4:Three dimensional plots of the complex refractive index.

It should be noted that some work has been performed on the use of polychromatic or spectroscopic ellipsometry to evaluate ion implantation dose concentration and uniformity. These works are provided in references 12-15. Future work in the realm of an optical evaluation of ion implantation should include this aspect, as it appears to be a significantly more powerful tool.

CONCLUSION

Although a relationship was clearly observed between the complex refractive index of the damaged layer and the dose concentration, by virtue of the increased distribution of the measured results, null ellipsometry using a HeNe laser source at a 70 degree incident angle, does not appear to be a feasible alternative to current ion implantation monitoring techniques. It was determined through an analysis of the variance that of the four factors evaluated, acceleration potential, dose concentration, and screen oxide thickness were statistically significant, while the forth factor, crystal orientation, was not. A potential alternative method for evaluating ion implantation may be spectroscopic ellipsometry.

ACKNOWLEDGMENTS

The author would like to thank the following people for there help. Mr. Paul Ballentine of CVC Products Inc. for the use of the CVC/Plasmos SD2000 Ellipsometer, Ms. Cheryl Christ of the Center for Quality Control and Applied Statistics at RIT for her help in setting up the experimental matrix, Dr. Joe Voelkel of the Center for Quality Control and Applied Statistics at RIT for his help in statistically analyzing the data, and Mr. Scott Blondell of RIT Microelectronic Engineering Facilities for his continual assistance in keeping the ion implanter running.

REFERENCES

[1] S. Wolf and R.N. Tauber, in Silicon Processing for the VLSI Era (Lattice Press, Sunset Beach, CA, 1986), pp. 280-330.
[2] H.S.W. Massey, E.W. McDaniel, B. Bederson, in Applied Atomic Collision Physics (Academic Press, Orlando, 1983), pp.545-575, pp.267-297.
[3] L. Wegmann, et al, Ion Implantation Science and Technology, edited by J.F. Ziegler (Academic Press, Orlando, 1984), pp. 51-210.
[4] G. Carter, W.A. Grant, in Ion Implantation of Semiconductors; (Wiley, New York, 1976), pp. 42-108.
[5] J.W. Mayer, L. Eriksson, J.A. Davies, in Ion Implantation in Semiconductors; Silicon and Germanium (Academic Press, London, 1970), pp. 65-124.
[6] O. Auciello, R. Kelly, in Ion Bombardment Modification of Surfaces; Fundamentals and Applications (Elsevier, Amsterdam, 1984), pp. 81-97.
[7] J. D. Hoepfner, Monitoring of X-Y-Scan Quality by Amorphization Contrast on Silicon Wafers (source unknown).
[8] A. K. Hochberg, The Measurement of Ion Implantation Doses in Silicon by Ellipsometry (source unknown).
[9] R.M.A. Azzam and N.M. Bashara, in Ellipsometry and Polarized Light, (Elsevier Science Publishers, Amsterdam, 1977), pp. 473-477.
[10] J.B. Schroeder and H.D. Dieselman, J. Appl. Phys. 40, 2559

(1969).
[11] P. Burggraf, Semiconductor International, November 1988, pp.76-83.
[12] F. Ferrieu, et al, J. Appl. Phys. 62, 3458 (1987).
[13] J.P. Cortot, P. Ged, Appl. Phys. Lett. 41, 93 (1982).
[14] P.J. McMarr, et al, J. Appl. Phys. 59, 694 (1986).
[15] S. Andrieu, et al, Antimony Adsorption on Silicon by In Situ Spectroscopic Ellipsometry Analysis (source unknown).

Real Component of the Refractive Index

1 Source	2 DF	3 SS	4 MS	5 F Value	6 Pr > F
E	2	0.030951	0.015475	0.67	0.5603
O	1	0.000009	0.000009	0.00	0.9853
E*O	2	0.070565	0.035283	1.53	0.3206
W (E*O)	4	0.092117	0.023029	10.17	0.0003
S	1	0.003667	0.003667	0.98	0.3780
E*S	2	0.277745	0.138872	37.15	0.0026
O*S	1	0.001556	0.001556	0.42	0.5539
E*O*S	2	0.007777	0.003889	1.04	0.4327
W (E*O*S)	4	0.014951	0.003738	1.65	0.2103
D	4	0.994142	0.248536	17.62	0.0001
E*D	8	0.955555	0.119444	8.47	0.0002
O*D	4	0.022128	0.005532	0.39	0.8113
E*O*D	8	0.189693	0.023712	1.68	0.1792
W (E*O*D)	16	0.225738	0.014109	6.23	0.0003

Imaginary Component of the Refractive Index

1 Source	2 DF	3 SS	4 MS	5 F Value	6 Pr > F
E	2	0.176396	0.088198	3.10	0.1538
O	1	0.001286	0.001286	0.05	0.8420
E*O	2	0.113619	0.056809	2.00	0.2504
W (E*O)	4	0.113804	0.028451	4.74	0.0102
S	1	0.273259	0.273259	132.14	0.0003
E*S	2	0.286388	0.143194	69.25	0.0008
O*S	1	0.029232	0.029232	14.14	0.0198
E*O*S	2	0.019663	0.009832	4.75	0.0877
W (E*O*S)	4	0.008272	0.002068	0.34	0.8437
D	4	0.910757	0.227689	9.19	0.0005
E*D	8	0.320655	0.040082	1.62	0.1963
O*D	4	0.051442	0.012860	0.52	0.7229
E*O*D	8	0.397213	0.049652	2.00	0.1126
W (E*O*D)	16	0.396337	0.024771	4.13	0.0036

TABLE 1: Analysis of variance.